

Synthesis and characterizations of charge-transfer complexes of 1,8-naphthalimides with different acceptors

M.S. Refat^{a,b*}, H. Al Didamony^c, Kh.M. Abou El-Nour^d, I. Grabchev^e, L. El-Zayat^a

^aDepartment of Chemistry, Faculty of Science, Port Said 42111, Port Said University, Egypt

^bDepartment of Chemistry, Faculty of Science, Taif University, 888 Taif, Kingdom Saudi Arabia

^cDepartment of Chemistry, Faculty of Science, Zagazig, Zagazig University, Egypt

^dDepartment of Chemistry, Faculty of Science, Ismailia, Suez Canal University, Egypt

^eUniversity of Sofia "St. Kliment Ohridski", Faculty of Medicine, 1407, 1 Koziak str, Sofia, Bulgaria

Received April 24, 2010; revised July 7, 2010

Five new Charge-Transfer (CT) complexes, formed from the of 4-substituted-N-allyl-1,8-naphthalimide derivatives as donors and σ -acceptor (iodine or π -acceptors) have been investigated. The data obtained indicate the formation of CT-complexes with the general formula of [(donors)(acceptor)_n], where n= 1 in the case of [(donors)I₂], [(donors)(DDQ)], [(donors)(CLA)], [(donors)(PA)] complexes and [(donors)(TCNQ)] except for [(4MAN)(TCNQ)₂], and [(4PAN)(TCNQ)₂] where n = 2.

Keywords: Charge-transfer; spectroscopic studies; acceptors; 1,8-naphthalimide.

INTRODUCTION

1,8-Naphthalimides and their 4-substituted derivatives are the subject of many scientific investigations, including laser active media [1,2], potential photosensitive biologically active units [3], fluorescent markers in biology [4], analgetics in medicine [5,6], collectors in solar energy [7]. Recently, they have been examined as fluorescent dichroic dyes in liquid crystals for utilization in electro-optical devices [8–10].

In the recent years, the charge-transfer complexes of organic species are intensively studied due to their special type of interaction, accompanied by transferring of an electron from the donor to the acceptor [11–15].

We undertook this work following our studies of the charge transfer complexes [16–24], in order to investigate spectrophotometrically the CT complexes formed from the 4-substituted-N-allyl-1,8-naphthalimide (4BAAN), 4-morpholino-N-allyl-1,8-naphthalimide (4MAN), 4-piperdino-N-allyl-1,8-naphthalimide (4PAN), 4-Methylamino-N-allyl-1,8-naphthalimide (4MAAN), and 4-

propyloxy-N-allyl-1,8-naphthalimide (4POAN)), as donors with σ -acceptors as iodine, and some π -acceptors (2,3-dichloro-5,6-dicyano-1,4-benzoquinone (DDQ), 7,7', 8,8'-tetracyanoquinodimethane (TCNQ), chloranilic acid (CLA) and picric acid (PA))

EXPERIMENTAL

Materials and Methods

All chemicals used in this study are Analar or extra pure grade.

Preparation of 1,8-naphthalimide derivatives

The syntheses of 4-substituted-N-allyl-1,8-naphthalimides presented in Fig. 1 have been described recently [25].

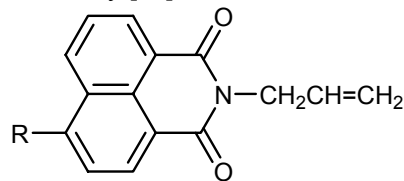


Fig. 1: General chemical structure of 1,8-naphthalimide derivatives, R = NHCH₂CH₂CH₂CH₃ (4-BAAN), Morpholino (4-MAN), Piperdino (4-PAN), NHCH₃ (4-MAAN) and OCH₂CH₂CH₃ (4-POAN).

* To whom all correspondence should be sent:

E-mail: msrefat@yahoo.com

Preparation of 1.8-naphthalimide charge-transfer complexes

Charge-transfer (CT) complexes, formed from the reactions between 4-substituted-N-allyl-1.8-naphthalimides and respective σ -acceptors, were synthesized as follows:

[4-Butylamino-N-allyl-1.8-naphthalimide]-I₂, DDQ, TCNQ, CLA and PA complexes

The charge-transfer complexes, [(4-BAAN)(Iodine)] (brown), [(4-BAAN)(DDQ)] (red), [(4-BAAN)(TCNQ)] (yellow crystal), [(4-BAAN)(CLA)] (yellow crystal), and [(4-BAAN)(PA)] (yellow crystal), were prepared by mixing 1 mmol of the donor in chloroform (10 ml) with 1 mmol of each of the acceptors, I₂, DDQ, TCNQ, CLA, and PA, in 10 ml of the same solvent with constant stirring for about 10 min. The solutions were allowed to evaporate slowly at a room temperature, the solids filtered and washed several times with little amounts of solvent, and dried under vacuum over anhydrous calcium chloride.

[4-Morpholino-N-allyl-1.8-naphthalimide]-I₂, DDQ, TCNQ, CLA and PA complexes:

The charge-transfer complexes, [(4-MAN)(Iodine)] (brown), [(4-MAN)(DDQ)] (red), [(4-MAN)(TCNQ)₂] (green), [(4-MAN)(CLA)] (red), and [(4-MAN)(PA)] (yellow), were prepared by mixing 1 mmol of the donor in chloroform (10 ml) with 1 mmol of each of the acceptors, I₂, DDQ, TCNQ, CLA, and PA, in 10 ml of the same solvent with constant stirring for about 10 min. The precipitate, formed in each of the cases, was filtered off immediately and washed several times with minimum amounts of chloroform, and dried under vacuum over P₂O₅.

[4-Piperidino-N-allyl-1.8-naphthalimide]-I₂, DDQ, TCNQ, CLA, and PA complexes

The charge-transfer complexes, [(4-PAN)(Iodine)] (brown), [(4-PAN)(DDQ)] (red), [(4-PAN)(TCNQ)₂] (yellow), [(4-PAN)(CLA)] (red), and [(4-PAN)(PA)] (yellow), were prepared by mixing 1 mmol of the donor in chloroform (10 ml) with 1 mmol of each of the f acceptors, I₂, DDQ, TCNQ, CLA, and PA, in 10 ml of the same solvent with constant stirring for about 10 min. The precipitate, formed in each of the cases, was filtered off immediately and washed several times with minimum amounts of chloroform, and dried under vacuum over P₂O₅.

[4-Methylamino-N-allyl-1.8-naphthalimide]-I₂, DDQ, TCNQ, CLA, and PA complexes

The charge-transfer complexes, [(4-MAAN)(Iodine)] (brown), [(4-MAAN)(DDQ)] (red), [(4-MAAN)(TCNQ)] (yellow), [(4-MAAN)(CLA)] (yellow), and [(4-MAAN)(PA)] (red), were prepared by mixing 1 mmol of the donor in chloroform (10 ml) with 1 mmol of each of the acceptors, I₂, DDQ, TCNQ, CLA, and PA, in 10 ml of the same solvent with constant stirring for about 10 min. The precipitate, formed in each of the cases, was filtered off immediately and washed several times with minimum amounts of chloroform, and dried under vacuum over P₂O₅.

[4-Propyloxy-N-allyl-1.8-naphthalimide]-I₂, DDQ, TCNQ, CLA, and PA complexes

The charge-transfer complexes, [(4-POAN)(Iodine)] (brown), [(4-POAN)(DDQ)] (red), [(4-POAN)(TCNQ)] (blue), [(4-POAN)(CLA)] (yellow), and [(4-POAN)(PA)] (yellow), were prepared by mixing 1 mmol of the donor in chloroform (10 ml) with 1 mmol of each of the acceptors, I₂, DDQ, TCNQ, CLA, and PA, in 10 ml of the same solvent with constant stirring for about 10 min. The precipitate, formed in each of the cases, was filtered off immediately and washed several times with minimum amounts of chloroform, and dried under vacuum over P₂O₅.

Instrumentation and physical measurements

The electronic spectra of donors, acceptors, and the respective CT complexes were recorded in the spectral region of 200-800 nm using a Jenway 6405 Spectrophotometer with quartz cells, 1.0 cm path in length. Photometric titration was performed at 25 °C for the reactions of the donors with the acceptors in chloroform, as follows: the concentration of the donors in the reaction mixtures was kept fixed at 5.0x10⁻⁴ M, while the concentration of the acceptors was changed over a wide range between Xx10⁻⁴ and Yx10⁻⁴ M. These produced solutions with donor/acceptor molar ratios, varying from 1: 0.25 to 1: 4.00.

FTIR measurements (KBr discs) of the donors, acceptor and CT complexes were carried out on a Bruker FT-IR spectrophotometer (400-4000 cm⁻¹). ¹HNMR spectra were obtained on Varian Gemini 200 MHz spectrometer. ¹HNMR data are expressed in parts per million (ppm), referenced internally to the residual proton impurity in DMSO (dimethylsulfoxide, d₆) as a solvent, and reported as chemical shift (m = multiplet and s = singlet; br =

broad). The complex compositions were confirmed by the mass spectra at 70 eV using AEI MS 30 mass spectrometer. We carried out the thermal analysis (TGA & DTG) out under nitrogen atmosphere at heating rate of 10 C/min using a Shimadzu TGA-50H thermal analyzers.

RESULTS AND DISCUSSION

The results of the elemental analysis for all CT complexes are listed in Table 1. The data shows that those values are in good agreement with the calculated ones, and the composition of the CT complexes is matched with the molar ratios, exhibited through the photometric titration, occurring between donors and acceptors (σ - and π -acceptors).

Table 1. Elemental analysis CHN and physical parameters data of the CT-complexes, formed from the reaction of the 4BAAN, 4MAN, 4PAN, 4MAAN, and 4POAN with iodine, DDQ, TCNQ, CLA, and PA.

Complexes (FW)	Mwt	C%		H%		N%		Physical data	
		Found	Calc.	Found	Calc.	Found	Calc.	Color	mp (°C)
[(4BAAN)]I ₂	562	40.32	40.57	3.50	3.56	4.88	4.98	Brown	95
[(4BAAN)(DDQ)]	535	60.23	60.56	3.56	3.73	8.87	8.97	Red	209
[(4BAAN)(TCNQ)]	512	72.19	72.61	4.56	4.68	16.25	16.40	Yellow	213
[(4BAAN)(CLA)]	517	57.85	58.02	4.18	4.25	5.39	5.41	Yellow	198
[(4BAAN)(PA)]	537	55.46	55.86	4.11	4.28	12.66	13.03	Yellow	168
[(4MAN)]I ₂	576	39.28	39.59	2.98	3.12	4.78	4.86	Brown	67
[(4MAN)(DDQ)]	549	58.94	59.01	3.19	3.46	10.09	10.20	Red	236
[(4MAN)(TCNQ) ₂]	731	70.19	70.63	3.48	3.56	18.98	19.16	Green	223
[(4MAN)(CLA)]	531	56.31	56.49	3.68	3.76	5.09	5.27	Red	216
[(4MAN)(PA)]	551	54.12	54.44	3.77	3.81	12.56	12.70	Yellow	184
[(4PAN)]I ₂	574	41.76	41.81	3.29	3.48	4.78	4.88	Brown	97
[(4PAN)(DDQ)]	547	61.11	61.42	3.78	3.84	10.11	10.23	Red	165
[(4PAN)(TCNQ) ₂]	729	72.32	72.47	3.65	3.84	18.98	19.21	Yellow	221
[(4-PAN)(CLA)]	529	58.73	58.98	4.08	4.16	5.09	5.29	Red	199
[(4PAN)(PA)]	549	56.28	56.83	4.13	4.19	12.69	12.75	Yellow	175
[(4MAAN)]I ₂	520	36.88	36.93	2.60	2.69	5.29	5.38	Brown	102
[(4MAAN)(DDQ)]	493	58.32	58.41	2.78	2.84	11.23	11.36	Red	196
[(4MAAN)(TCNQ)]	470	71.39	71.49	3.99	4.04	17.75	17.87	Yellow	187
[(4MAAN)(CLA)]	475	55.09	55.58	3.29	3.37	5.75	5.89	Yellow	149
[(4MAAN)(PA)]	495	53.25	53.33	3.37	3.43	13.95	14.14	Red	166
[(4POAN)]I ₂	549	39.11	39.36	2.89	3.09	2.51	2.55	Brown	85
[(4POAN)(DDQ)]	522	59.38	59.77	3.16	3.25	7.95	8.04	Red	239
[(4POAN)(TCNQ)]	499	72.08	72.14	4.15	4.21	13.85	14.03	Blue	211
[(4POAN)(CLA)]	504	57.03	57.14	3.62	3.77	2.56	2.78	Yellow	166
[(4POAN)(PA)]	524	54.66	54.96	3.76	3.81	10.65	10.68	Yellow	163

Electronic absorption spectra

The absorption UV/Vis spectra of the 1,8-naphthalimide/iodine complexes were measured in CHCl₃. The complexes are formed with donors (4BAAN, 4MAN, 4PAN, 4MAAN and 4POAN) by adding X ml of 5.0×10⁻⁴ M (I₂) (X = 0.25, 0.50, 0.75, 1.00, 1.50, 2.00, 2.50 and 3.00 ml) to 1.00 ml of 5.0×10⁻⁴ M of each donor. The volume of the

mixtures in each case was adjusted to 10 ml in each donor. The donor concentration in the reaction mixtures was kept fixed at 0.5×10⁻⁴ M, while the iodine concentration varied in the range between 0.125×10⁻⁴ M and 1.50×10⁻⁴ M. These concentrations produced base to I₂ ratios within the range between 1:0.25 and 1:3.00. The electronic absorption spectra of the reactants of I₂ and 4BAAN, 4MAN, 4PAN, 4MAAN, and 4POAN

mixed with CHCl_3 in a volumetric ratio of 1:1 are

shown in Figures (2A-E), respectively. The spectra

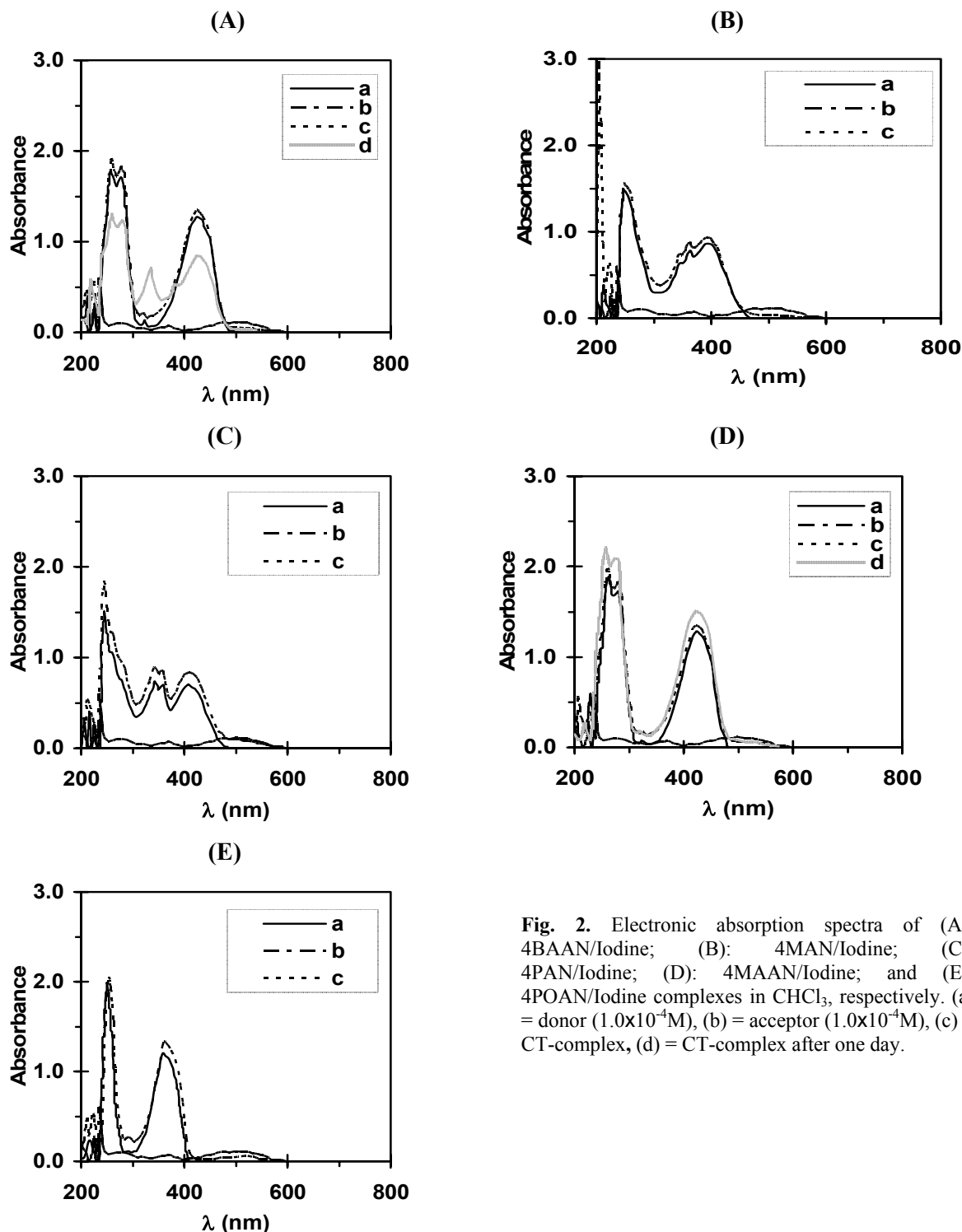


Fig. 2. Electronic absorption spectra of (A): 4BAAN/Iodine; (B): 4MAN/Iodine; (C): 4PAN/Iodine; (D): 4MAAN/Iodine; and (E): 4POAN/Iodine complexes in CHCl_3 , respectively. (a) = donor ($1.0 \times 10^{-4} \text{M}$), (b) = acceptor ($1.0 \times 10^{-4} \text{M}$), (c) = CT-complex, (d) = CT-complex after one day.

show detected absorption bands. These bands are assigned at (335, 385 and 505 nm), (390 and 505 nm), (410 and 510 nm), (425 and 500 nm), and at (360 and 500 nm) due to the CT complex, formed in the reaction of 4BAAN, 4MAN, 4PAN,

4MAAN, and 4POAN with I_2 in solvent chloroform, respectively. The photometric titration curves were obtained adhering to the molar ratio method [27], by plotting of the absorbance against the volume of the iodine σ -acceptor added. The

equivalence points, shown on these curves, clearly indicate that the CT-complex, formed between the donor (4BAAN, 4MAN, 4PAN, 4MAAN and 4POAN) and the iodine, is in a 1:1 ratio. The formation of 1:1 complex was strongly supported by elemental analysis, photometric titrations and far infrared spectra. The spectrophotometric data are employed to calculate the equilibrium constant (K_{CT}) and the molar absorbance (ϵ_{CT}) for donor- I_2 complexes in chloroform using the 1:1 modified Benesi-Hildebrand equation [28]. This equation is based on the assumptions of 1:1 (Acceptor-Donor) complex formation. Calculations are based on the data obtained for, C_D^0 of (4BAAN, 4MAN, 4PAN, 4MAAN and 4POAN), C_A^0 of I_2 , $C_A^0 + C_D^0$ and $C_A^0 \times C_D^0 / A$ in $CHCl_3$. When the $C_A^0 \times C_D^0 / A$ values for each donor are plotted against the corresponding $C_A^0 + C_D^0$ values, the straight lines are obtained with a slope of $1/\epsilon$ and intercept of $1/K\epsilon$ for the reactions in $CHCl_3$. Both, the equilibrium constant (K) and the molar absorbance (ϵ) for all CT complexes, are given in Table 2. The value trend in this table reveals high values of both, the equilibrium constant (K) and the molar absorbance (ϵ). This high value of (K) reflects the high stability of the iodine complexes because of the expected high donation of the 4-butylamino for (4BAAN), the 4-morpholino for (4MAN), the 4-piperidino for (4PAN), the 4-methylamino for (4MAAN), and the 4-propyloxy for (4POAN) N-allyl derivatives of 1.8-naphthalimide (donor).

The CT transition energies of CT- complexes are used to estimate the ionization potential of (4BAAN, 4MAN, 4PAN, 4MAAN and 4POAN) using the empirical equations, derived by Aloisi and Pignataro [29]. The values obtained are listed in Table 2.

The electronic absorption spectra of the free donors, 4BAAN, 4MAN, 4PAN, 4MAAN and 4POAN with DDQ in chloroform along with those of the formed 1:1 CT complexes, are shown on Figures (3 A-E), respectively. The spectra demonstrate that the formed CT-complexes show new absorption bands which do not exist in the spectra of the reactants. These bands are attributed to charge-transfer complexes formation and can be assigned as follows: 360 and 430 nm for 4BAAN/DDQ, 360 and 390 nm for 4MAN/DDQ, 357 and 410 nm for 4PAN/DDQ, 355 and 425 nm for 4MAAN, and (355 and 410 nm) for 4POAN/DDQ, respectively. In the measurements the concentration of the donors (4BAAN, 4MAN, 4PAN) was kept fixed at 0.25×10^{-4} M while the concentration of the acceptor varied in the range of

0.0625×10^{-4} M to 0.75×10^{-4} M. The concentration of the other donors (4MAAN and 4POAN) was kept fixed at 0.50×10^{-4} M while the concentration of the acceptor varied in the range of 0.125×10^{-4} M to 1.50×10^{-4} M. Accordingly, the CT-complexes, formed upon the reaction of 4BAAN, 4MAN, 4PAN, 4MAAN and 4POAN as donors with π -acceptor DDQ under investigation, have the general formula of [(donor)(acceptor)]. The 1:1 modified Benesi-Hildebrand equation [28] was used as shown in the previous sections in the calculation of the values of the equilibrium constant, K , and the molar absorbance, ϵ . While plotting the $C_A^0 \cdot C_D^0 / A$ values against the $C_A^0 + C_D^0$ values for the donors/DDQ, straight lines were obtained with a slope of $1/\epsilon$ and an intercept of $1/K\epsilon$. The obtained values of both K and ϵ , associated with these complexes, are given in Table 3.

Figures 4 (A-E) show the electronic absorption spectra of the reactant donors, 4BAAN, 4MAN, 4PAN, 4MAAN and 4POAN, with TCNQ in chloroform along with the 1:1 molar ratio of donor: acceptor with 4BAAN, 4MAAN, and 4POAN, while the molar ratio for donor: acceptor is 1:2 for the donors of 4PAN and 4MAAN. The spectra demonstrate that the formed CT complexes show new absorption bands at 410 and 455 nm for the 4BAAN/TCNQ, 410 nm for the 4MAN/TCNQ, 405 nm for the 4PAN/TCNQ, 405 and 450 nm for the 4MAAN/TCNQ, and (355 and 405 nm) for the 4POAN/TCNQ, respectively. The concentration of donors (4BAAN and 4MAN) in these measurements was kept fixed at 0.50×10^{-4} M while the concentration of the TCNQ varied in the range of 0.125×10^{-4} M to 1.50×10^{-4} M. The concentration of 4PAN donor was kept fixed at 0.125×10^{-4} M while the concentration of the TCNQ varied in the range of 0.031×10^{-4} M to 0.50×10^{-4} M. In the case of the donors (4MAAN and 4POAN) the concentration was kept fixed at 0.25×10^{-4} M while the concentration of the TCNQ varied in the range of 0.0625×10^{-4} M to 0.75×10^{-4} M. Accordingly, the CT complexes, formed upon the reaction of 4BAAN, 4MAN, 4PAN, 4MAAN and 4POAN, being the donors with TCNQ under investigation, have the formula of [(4BAAN)(TCNQ)], [(4MAN)(TCNQ)₂], [(4PAN)(TCNQ)₂], [4MAAN)(TCNQ)] and [(4POAN)(TCNQ)] CT complexes. The 1:1 modified Benesi-Hildebrand equation [28] was used to calculate the values of the equilibrium constant, K ($l \text{ mol}^{-1}$), and the molar absorptivity, ϵ ($l \text{ mol}^{-1} \text{ cm}^{-1}$), for the [(4BAAN)(TCNQ)], the [4MAAN)(TCNQ)] and

the [(4POAN)(TCNQ)] CT complexes. The corresponding spectral parameters for the complexes of [(4MAN)(TCNQ)₂] and [(4PAN)(TCNQ)₂], were calculated using the known El-Kourashy equation [30] for 1:2 complexes.

Here, C_A^0 and C_D^0 are the initial concentration of the TCNQ and the donors, respectively, while A is the absorbance at the mentioned CT bands. Straight lines are obtained with a slope of $1/\epsilon$ and intercept of $1/K\epsilon$ when plotting the values of $C_A^0 C_D^0 / A$ against the $(C_A^0 + C_D^0)$ values, and the

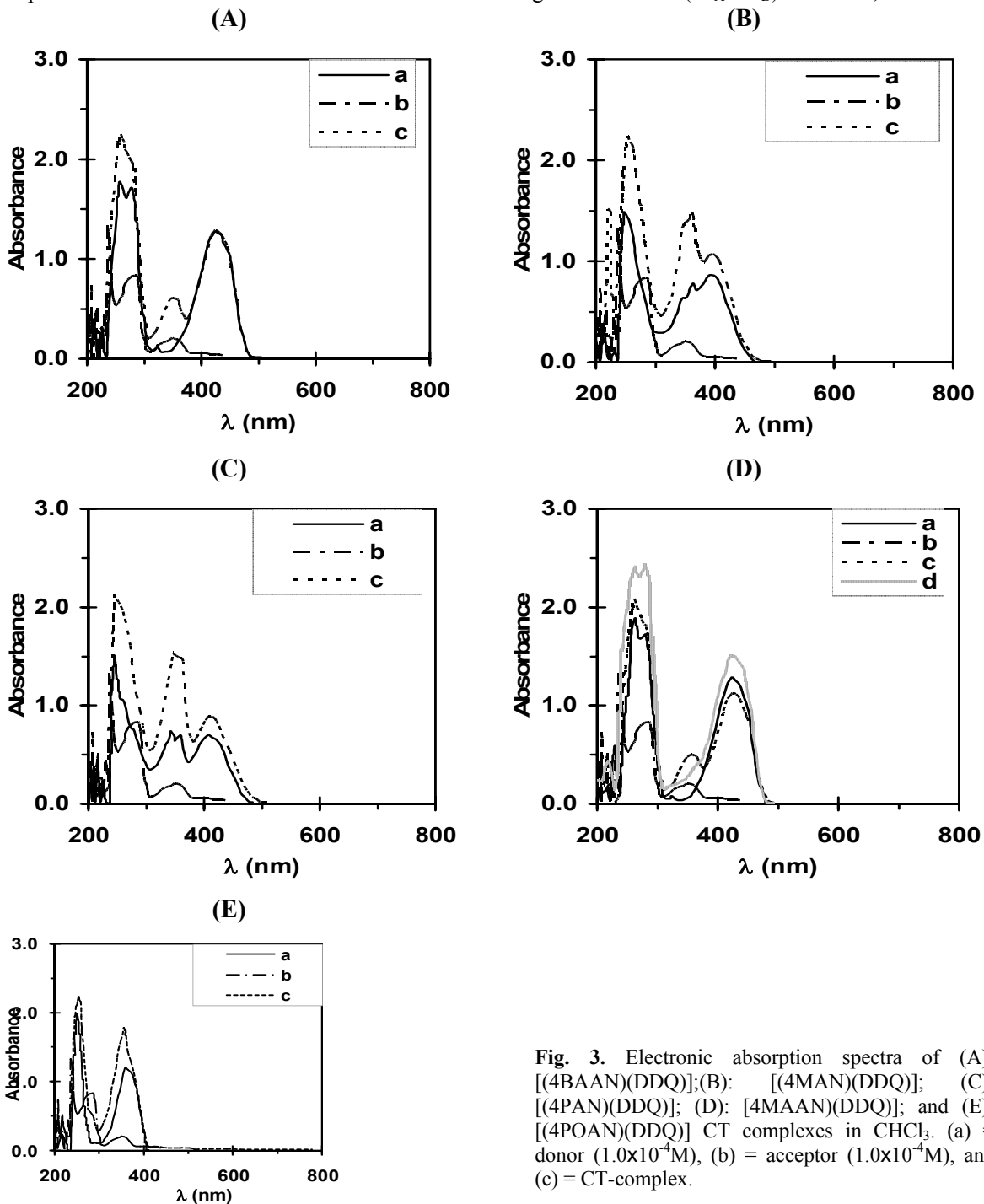


Fig. 3. Electronic absorption spectra of (A): [(4BAAN)(DDQ)];(B): [(4MAN)(DDQ)]; (C): [(4PAN)(DDQ)]; (D): [4MAAN)(DDQ)]; and (E): [(4POAN)(DDQ)] CT complexes in CHCl₃. (a) = donor (1.0x10⁻⁴M), (b) = acceptor (1.0x10⁻⁴M), and (c) = CT-complex.

values of $(C_A^0)^2 C_D^0 / A$ versus the $C_A^0 (C_A^0 + 4C_D^0)$ values. Table 4 shows the calculated values of the

spectroscopic data, containing the ϵ , K and I_p .

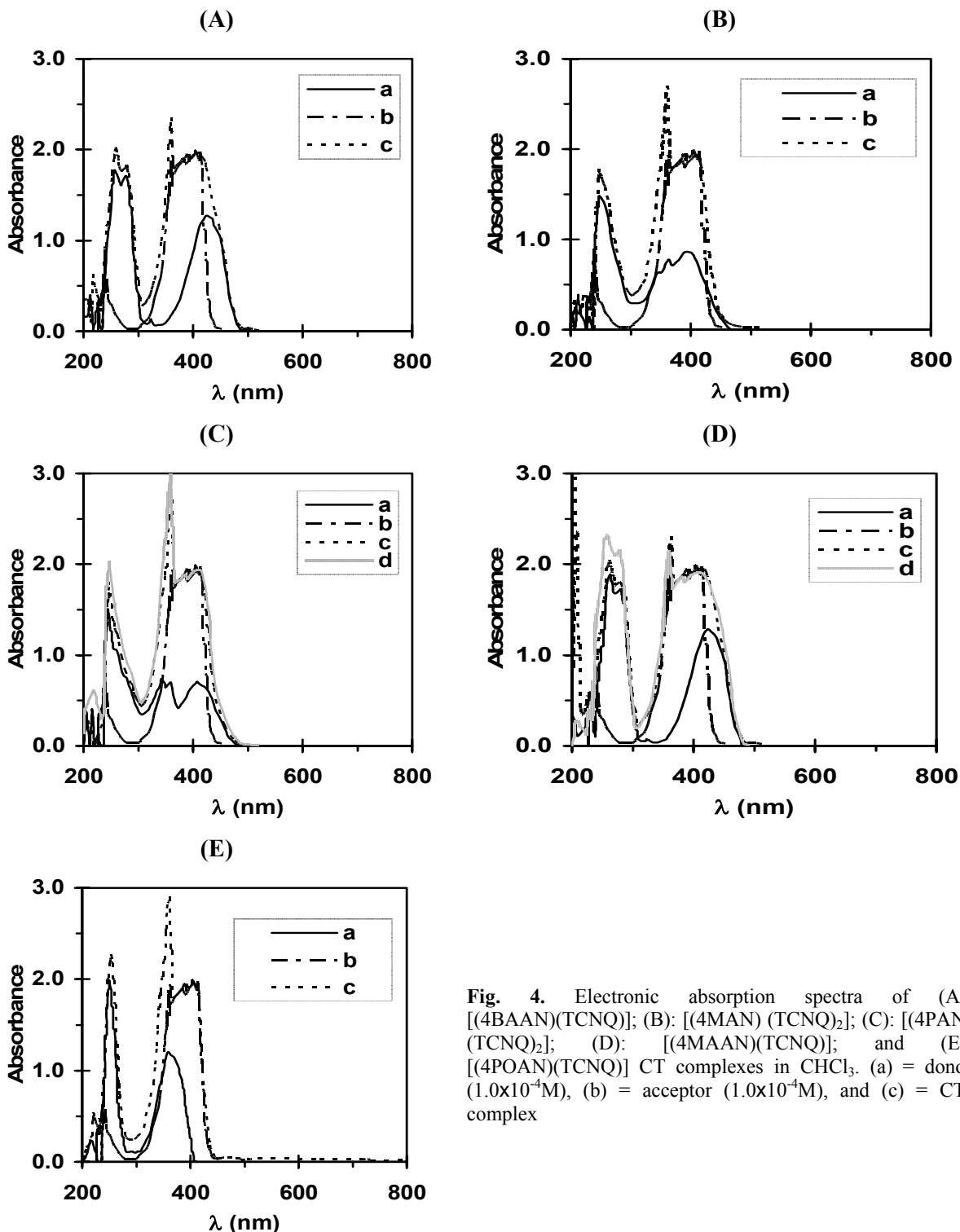


Fig. 4. Electronic absorption spectra of (A): [(4BAAN)(TCNQ)]; (B): [(4MAN)(TCNQ)₂]; (C): [(4PAN)(TCNQ)₂]; (D): [(4MAAN)(TCNQ)]; and (E): [(4POAN)(TCNQ)] CT complexes in CHCl₃. (a) = donor (1.0x10⁻⁴M), (b) = acceptor (1.0x10⁻⁴M), and (c) = CT-complex

The electronic absorption spectra of the reactant donors of 4BAAN, 4MAN, 4PAN, 4MAAN, and 4POAN with CLA in CH₃OH along with those of the formed 1:1 CT complexes are shown on Figure 5. The

spectra demonstrate that the formed CT complexes show new absorption bands as follows: at 320 and 525 nm for the 4BAAN/CLA, 310 and 520 nm for the 4MAN/CLA, 315 and 535 nm for the 4PAN/CLA,

general formula of [(donor)(acceptor)]. The 1:1 modified Benesi-Hildebrand equation was used as shown in the previous sections for the calculation of the values of the equilibrium constant, K , and the molar absorptivity, ϵ . Straight lines are obtained with

a slope of $1/\epsilon$ and an intercept of $1/K\epsilon$. Table 5 shows the obtained values of both, K and ϵ , associated with these complexes.

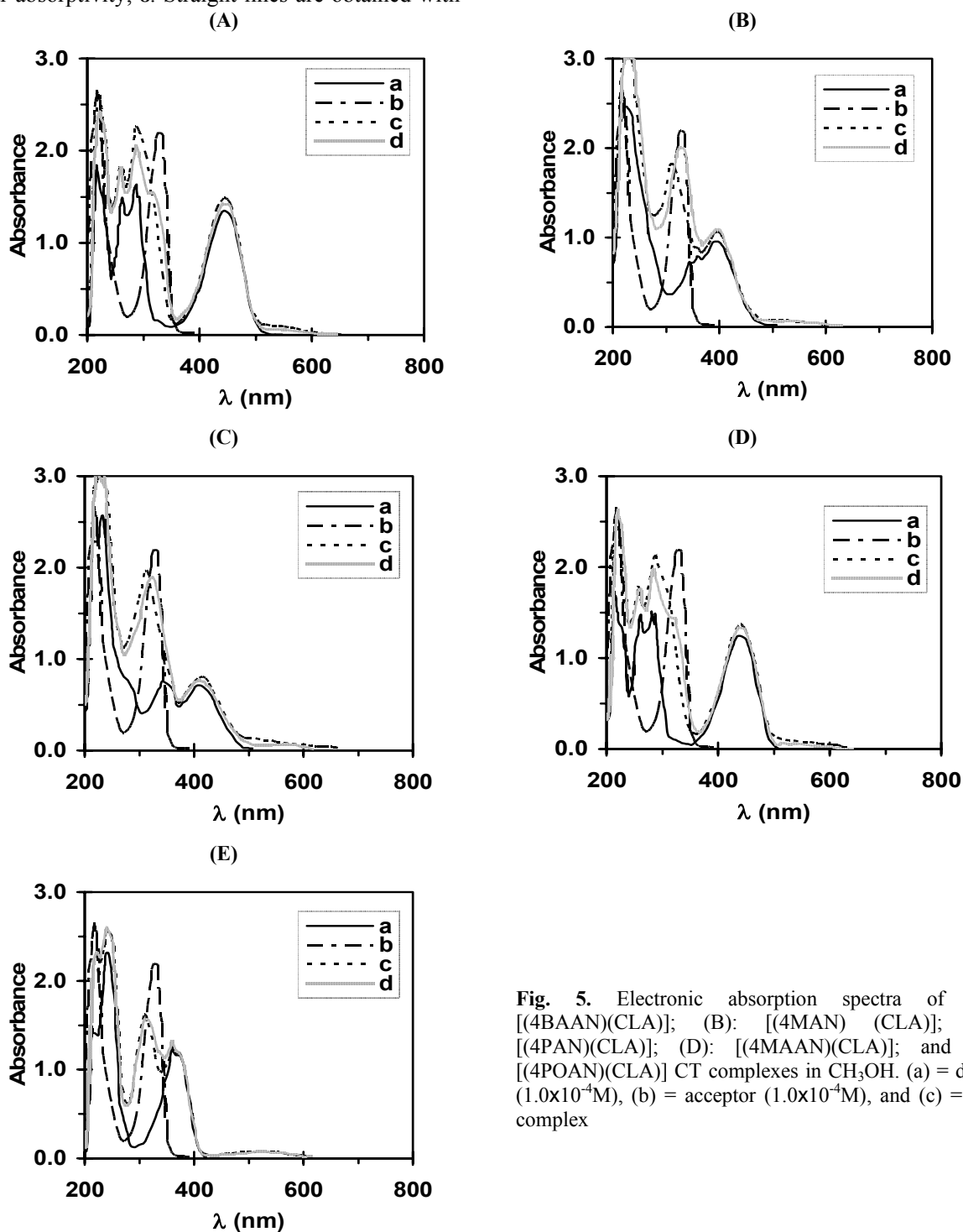


Fig. 5. Electronic absorption spectra of (A): [(4BAAN)(CLA)]; (B): [(4MAN)(CLA)]; (C): [(4PAN)(CLA)]; (D): [(4MAAN)(CLA)]; and (E): [(4POAN)(CLA)] CT complexes in CH_3OH . (a) = donor ($1.0 \times 10^{-4}\text{M}$), (b) = acceptor ($1.0 \times 10^{-4}\text{M}$), and (c) = CT-complex

Table 2: Spectrophotometric results for (A): 4BAAN/iodine; (B): 4MAN/iodine; (C): 4PAN/iodine; (D): 4MAAN/iodine; and (E): 4POAN/iodine CT complexes.

CT-complexes	λ_{\max} (nm)	E_{CT} (eV)	K ($l.mol^{-1}$)	ϵ_{\max} ($l.mol^{-1}.cm^{-1}$)	I_p
A	385	3.23	2.06×10^4	2.36×10^4	7.37
B	390	3.19	2.22×10^4	2.85×10^4	7.35
C	410	3.03	2.19×10^4	2.06×10^4	7.23
D	425	2.93	2.12×10^4	2.74×10^4	7.16
E	360	3.45	2.07×10^4	4.96×10^4	7.53

Table 3: Spectrophotometric results for (A): [(4BAAN)(DDQ)]; (B): [(4MAN)(DDQ)]; (C): [(4PAN)(DDQ)]; (D): [(4MAAN)(DDQ)]; and (E): [(4POAN)(DDQ)] CT complexes.

CT complexes	λ_{\max} (nm)	E_{CT} (eV)	K ($l.mol^{-1}$)	ϵ_{\max} ($l.mol^{-1}.cm^{-1}$)	I_p
A	430	2.89	4.30×10^4	3.34×10^4	7.14
B	390	3.18	4.15×10^4	4.97×10^4	7.34
C	410	3.03	4.08×10^4	4.97×10^4	7.23
D	425	2.93	2.35×10^4	3.26×10^4	7.16
E	410	3.03	2.49×10^4	0.816×10^4	7.23

Table 4: Spectrophotometric results for (A): [(4BAAN)(TCNQ)]; (B): [(4MAN)(TCNQ)₂]; (C): [(4PAN)(TCNQ)₂]; (D): [4MAAN)(TCNQ)]; and (E): [(4POAN)(TCNQ)] CT complexes.

CT complexes	λ_{\max} (nm)	E_{CT} (eV)	K ($l.mol^{-1}$)	ϵ_{\max} ($l.mol^{-1}.cm^{-1}$)	I_p
A	455	2.73	2.21×10^4	1.61×10^4	7.02
B	410	3.03	1.68×10^8	9.47×10^4	7.23
C	405	3.07	34.99×10^8	3.93×10^5	7.26
D	450	2.76	4.87×10^4	2.51×10^4	7.04
E	405	3.07	7.84×10^4	11.28×10^4	7.26

Table 5: Spectrophotometric results for (A): [(4BAAN)(CLA)]; (B): [(4MAN)(CLA)]; (C): [(4PAN)(CLA)]; (D): [4MAAN)(CLA)]; and (E): [(4POAN)(CLA)] CT complexes.

CT complexes	λ_{\max} (nm)	E_{CT} (eV)	K ($l.mol^{-1}$)	ϵ_{\max} ($l.mol^{-1}.cm^{-1}$)	I_p
A	525	2.73	10.61×10^4	0.996×10^4	7.02
B	520	2.39	10.88×10^4	0.389×10^4	6.79
C	535	2.32	3.15×10^4	0.901×10^4	6.74
D	530	2.34	7.83×10^4	0.470×10^4	6.75
E	520	2.39	21.36×10^4	0.692×10^4	6.79

The electronic absorption spectra of the donors, 4BAAN, 4MAN, 4PAN, 4MAAN and 4POAN with PA in $CHCl_3$ along with those of the formed 1:1 CT complexes are shown on Figure 6. The spectra demonstrate that the formed CT complexes show new absorption bands as follows: 335 and 425 nm for the 4BAAN/PA, 340 and 400 nm for

the 4MAN/PA, 330 and 410 nm for the 4PAN/PA, 335 and 425 nm for the 4MAAN/PA, and 360 and 430 nm for the 4POAN/PA. In these measurements the concentration of the donors (4BAAN, 4MAN, 4PAN, 4MAAN and 4POAN) was kept fixed at 0.25×10^{-4} M while the concentration of the PA was in the range of 0.0625×10^{-4} M to 0.75×10^{-4} M.

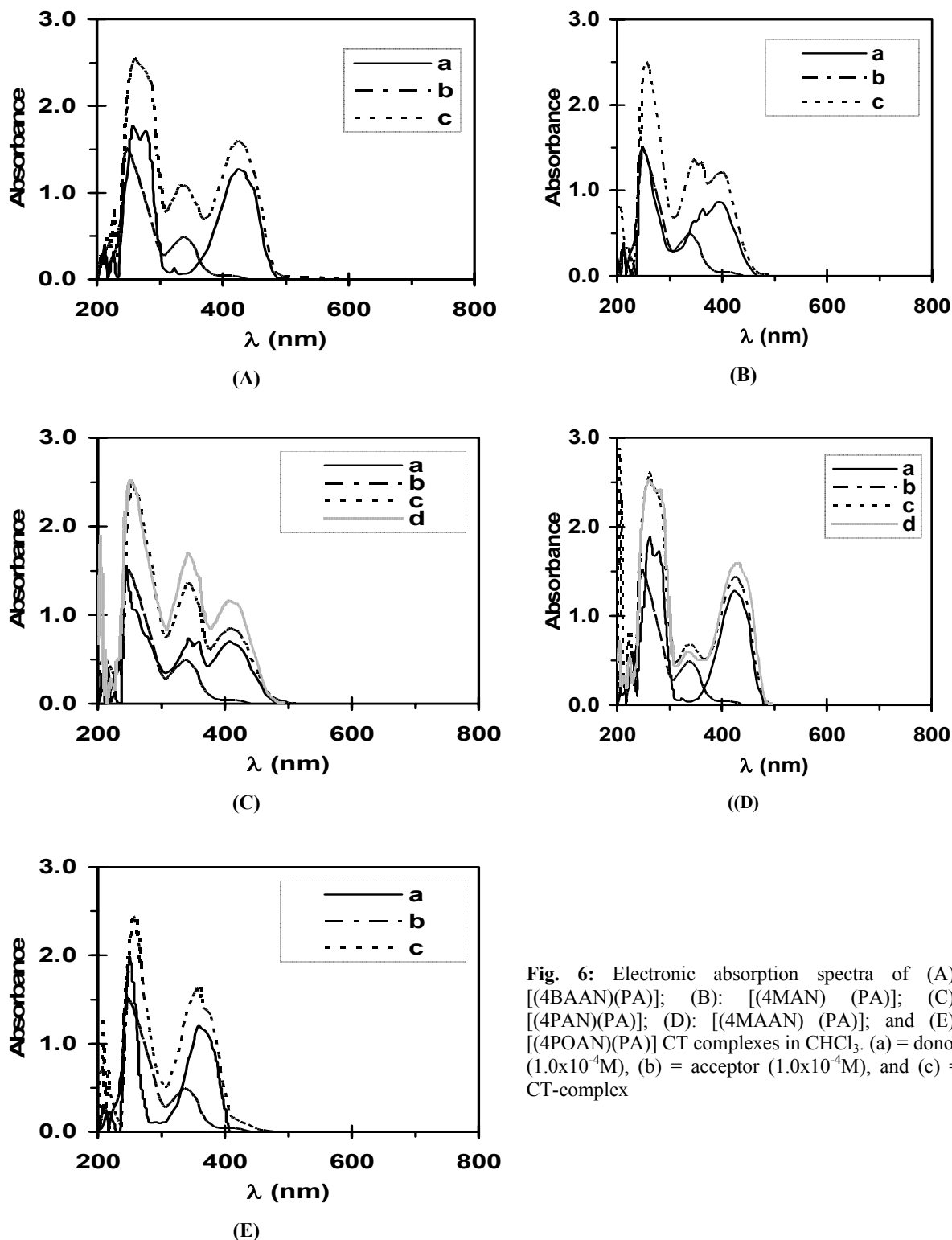


Fig. 6: Electronic absorption spectra of (A): [(4BAAN)(PA)]; (B): [(4MAN) (PA)]; (C): [(4PAN)(PA)]; (D): [(4MAAN) (PA)]; and (E): [(4POAN)(PA)] CT complexes in CHCl_3 . (a) = donor ($1.0 \times 10^{-4} \text{M}$), (b) = acceptor ($1.0 \times 10^{-4} \text{M}$), and (c) = CT-complex

Accordingly, the CT-complexes, formed upon the reaction of 4BAAN, 4MAN, 4PAN, 4MAAN and 4POAN, being the donors with PA under investigation, have the general formula of

[(donor)(acceptor)]. The 1:1 modified Benesi-Hildebrand equation was used in the calculation of the values of the equilibrium constant, K , and the molar absorptivity, ϵ . The values C_a^0 and C_d^0 are

the initial concentrations of the PA and the donors of 4BAAN, 4MAN, 4PAN, 4MAAN and 4POAN, respectively, while A is the absorbance at the CT bands. A straight line with a slope of $1/\varepsilon$ and intercept of $1/K\varepsilon$ is obtained when plotting the values of the $C_a^0 \cdot C_d^0/A$ against the $C_a^0 + C_d^0$ values for

each donor. The obtained values of both, K and ε , associated with these complexes, are given in Table 6. These complexes show high values of both the formation constants (K) and the molar absorptivity (ε). These high values of K confirm the expected high stabilities of the formed CT complexes.

Table 6: Spectrophotometric results for (A): [(4BAAN)(PA)]; (B): [(4MAN)(PA)]; (C): [(4PAN)(PA)]; (D): [(4MAAN)(PA)]; and (E): [(4POAN)(PA)] CT complexes.

CT complexes	λ_{\max} (nm)	E_{CT} (eV)	K (l.mol^{-1})	ε_{\max} ($\text{l.mol}^{-1} \cdot \text{cm}^{-1}$)	I_p
A	425	2.93	4.32×10^4	3.75×10^4	7.16
B	400	3.11	4.21×10^4	4.73×10^4	7.29
C	410	3.03	4.50×10^4	4.21×10^4	7.23
D	425	2.93	4.44×10^4	3.98×10^4	7.16
E	430	2.90	5.35×10^4	2.27×10^4	7.14

Infrared spectra

The FTIR spectra of 4BAAN, 4MAN, 4PAN, 4MAAN and 4POAN and the respective CT complexes of [(4BAAN)]₂, [(4MAN)]₂, [(4PAN)]₂, [(4MAAN)]₂ and [(4POAN)]₂ were recorded at KBr and data are listed in Table 7. As expected, the band characteristics for the 4BAAN, 4MAN, 4PAN, 4MAAN and 4POAN units in [(donor)]₂ CT-complexes are shown with small changes in band intensities and frequency values, indicating the formation of the charge-transfer complexes.

The far infrared spectra of [(4BAAN)]₂, [(4MAAN)]₂ and [(4POAN)]₂ CT complexes were recorded from Nujol mulls, dispersed on polyethylene windows in the region of 50-300 cm^{-1} . The absence of the bands, characteristic for I_3^- in the spectra show the formation of the [(donor)]₂ CT-complexes.

The infrared characteristic bands of the CT complexes, formed from the interaction of the 1,8-naphthalimide with (acceptor = DDQ, TCNQ, CLA and PA), are assignments and are given in Tables (8 to 11). These assignments are based on the comparison between the spectra of CT complexes and the spectra of the reactants, the donors and the acceptors. The spectra of the reaction products contain the main bands for both reactants, and this strongly supports the formation of the CT-complexes. However, the bands of the acceptors and the donor in the spectra of 1,8-naphthalimide CT complexes show some changes in the intensities and in some cases show small shifts in the frequency values, compared to those of the free acceptors and the donor. This could be understood based on the symmetry and the

electronic structure changes in both, the acceptors and the donors in the formed CT-complexes, compared to those of the free molecules.

The comparison between the important IR spectral bands of the free donors of N-allyl derivatives of 1,8-naphthalimide and the π -acceptor DDQ and the corresponding bands, appearing in the IR spectra of the prepared CT complexes, shows strong patterns due to the corresponding radical anions, DDQ \cdot^- . Essentially, the vibration frequencies of the C \equiv N groups for DDQ, observed at 2250 and 2231 cm^{-1} , are shifted to lower wavenumbers of 2213-2237 cm^{-1} in the corresponding IR spectra of its CT complexes with 1,8-naphthalimide (4BAAN, 4MAN, 4PAN, 4MAAN, and 4POAN). Also, the stretching vibration frequencies of the C=O groups, appearing at 1673 cm^{-1} in the IR spectrum of free DDQ, is displayed at 1635-1655 cm^{-1} and 1678-1698 cm^{-1} in their complexes. Furthermore, the bands belonging to the C-Cl vibrations which appeared at 800 and 720 cm^{-1} in the IR spectra of the free DDQ, exhibit a high shift in the corresponding IR spectra of the CT complexes (at 894-885 and 744-783 cm^{-1}). Accordingly, these interpretation led to the deduction that the CT complexation occurs as π - π^* (aromatic ring of donor to aromatic ring of acceptor), see Scheme 1. The IR spectral bands of the [(4BAAN)(TCNQ)], [(4MAN)(TCNQ)]₂, [(4PAN)(TCNQ)]₂, [(4MAAN)(TCNQ)] and the [(4POAN)(TCNQ)] solid CT complexes are given in Table 9. The structures of the 1,8-naphthalimide/TCNQ CT complexes,

Table 7: Infrared frequencies^(a) (cm⁻¹) and tentative assignments for (A): 4BAAN; (B): 4MAN; (C): 4PAN; (D): 4MAAN; (E): 4POAN; (F): 4BAAN/iodine; (G): 4MAN/iodine; (H): 4PAN/iodine; (I): 4MAAN/iodine; and (J): 4POAN/iodine complexes in CHCl₃, respectively.

A	B	C	D	E	[(Donors)]I ₂					Assignments ^(b)
					F	G	H	I	J	
3382 s	--	--	3391 vs	3424 w,br	3391 w 3336 w	--	--	3389 s 3321 w	3424 br	v(O-H); H ₂ O of KBr v(N-H)
3075 w	3072 w	3071 w 3010 w	3085 vw	3078 w	3079 vw	--	3076 w	3058 vw	3078 w	v _{as} (C-H); aromatic v(C-H); CH ₂ +CH ₃
2955 ms	2952 m	2934 ms	2989 vw	2964 ms	2923 m	2925 vs	2925ms	2929 m	2962 ms	v _s (C-H)
2867 m	2895 w 2846ms	2850 m 2812 m	2930 w 2851vw	2938 w 2876 mw	2856 w	2854 s	2853 m		2928 ms 2874 w	v _{as} (C-H)
1682 s	1690 s	1697 s	1681 s	1697 s	1673 s	1741 s	1698 ms	1682 s	1696 s	v(C=O)
1642 vs	1656 vs	1652 vs	1637 s	1659 vs	1608 ms	1699 s	1656 s	1635 s	1658 vs	
1612 vw	1588 s	1590 s 1512 m	1577 vs 1549 s	1590 s 1514 ms	1580 vs	1582ms 1515 m	1582 s 1514 m	1579 vs 1548 s 1528 w	1590 s 1590 s 1522 ms	v(C=C); aromatic
1577 vs	1512 m	1447 vw	1446 m	1461 ms	1550 ms	1458 ms	1459 m	1478 w	1460 ms	δ(CH); CH def.
1544 vs	1448 m	1452 mw	1418 m	1380 s	1523 s	1375 ms	1423 w	1451 w	1422 m	δ(CH); aromatic
1470 m	1380 s	1381 ms	1380 s		1470 ms 1376 m		1375 s 1340 m	1380 s	1379 s	
1335 s	1342 ms	1235 ms 1235 s	1355 ms 1299 ms	1327 vw 1269 s	1345 ms 1279 w	1340 w 1235 ms	1234 ms 1156vw	1353 s 1299 w	1267 s 1233 s	v(C-C) v(C-N)
1294 ms	1238 s	1178 m	1245 ms	1234 s	1248 s	1161 m	1130 w	1276 w	1182 w	v(C-O)
1247 s	1179 ms	1134 m	1155 ms	1185 m	1191 w	1117 m	1078 w	1246 ms	1137 m	CH, in-plane bend
1187 w	1118 s 1078 m	1080 mw	1090 w	1136 m	1165 s			1166 ms	1099 w	
1097 m			1060 vw	1100 ms	1044 w			1056 m	1076 m	
1023 w	1021 w	1019 w	1023 vw	1026 m	977 ms	1031 w	982 w	976 ms	1026 vw	δ _{rock} ; NH CH-deformation
979 m	983 ms	975 mw	946 vw	995 ms	891 w	983 w	931 w	947 w	995 m	
940 w	942 w	952 vw	819 w	927 ms	854 w	927 w	855 m	893 vw	927 m	
916 w	883 m	851 m	770 s	832 ms	823 w	857 w	773 vs	815 w	830 ms	
827 w	844 ms	780 s	695 vw	780 s	766 ms	772 vs		769 s	779 s	
779 s	785 s 757 ms	717 vw	656 vw	756 m				694 w		
673 vw	677 w	691 vw		668 m	655 w	673 vw	607 vw	583 m	668 m	Skeletal vibration
584 m	629 w 562 w 501 w	625 vw 564 vw	581 m 522 m	630 w 581 w	585 m	599 vw	564 w 492 w	531 m 498 w	615 w 577 w	CH bend
507 m	417 ms	464 vw	467 vw	496 w	501 m	417 m	464 w	466 w	494 w	CH out of plane bend
467 w		419 m	420 w	457 w 410 m	438 vw		422 m	420 w	460 w 415 w	Skeletal vibration CNC def.

(a): s = strong, w = weak, m = medium, sh = shoulder, v = very, br = broad.

(b): v, stretching; δ, bending.

are strongly supported by the observed main infrared bands for the reactants. However, the bands of 1,8-naphthalimide derivatives and TCNQ in the spectra of the [(4BAAN)(TCNQ)], [(4MAN)(TCNQ)₂], [(4PAN)(TCNQ)₂], [(4MAAN)(TCNQ)], and [(4POAN)(TCNQ)] complexes show small

shifts in the frequency values as well as some changes in their intensities in comparison to those of the free donors and the TCNQ. This could be attributed to the expected symmetry and electronic structure changes in the formation of the CT complexes. In the case of the In the case of the [(4MAN)(TCNQ)₂] and

Table 8: Infrared frequencies^(a) (cm⁻¹) and tentative assignments for (A): [(4BAAN)(DDQ)]; (B): [(4MAN)(DDQ)]; (C): [(4PAN)(DDQ)]; (D): [(4MAAN)(DDQ)]; and (E): [(4POAN)(DDQ)] CT complexes.

A	B	C	D	E	Assignments ^(b)
3248 s, br	3421 w, br 3227 w,br	3226 vs,br	3388 ms 3236 ms, br	3423 ms,br 3240 w ,br	v(O-H); and H ₂ O of KBr v(N-H)
2978 vw 2945 vw	2982 w	2932 ms	2925 vw	2966 ms	v _{as} (C-H); CH ₂ +CH ₃ v(C-H); aromatic
2838 vw	2951 mw 2845 m	2854 w	2849 vw	2879 w	v _s (C-H) + v _{as} (C-H)
2251 s	2213 s	2251 ms	2237 ms	2231 ms	v(C≡N); DDQ
1680 w 1635 ms	1691 s 1655 vs	1698 s 1655 vs	1678 ms 1637 s	1694 s 1652 vs	v(C=O); DDQ + donors
1576 s	1584 vs	1581 vs 1514 w	1577 vs 1549 w	1587 s 1517 m	v(C=C); aromatic
1452 vs	1450 ms 1380 s	1452 vs 1376 s	1451 s 1421 w 1379 ms	1454 ms 1382 s	δ(CH); CH _{def} . δ(CH); aromatic
1359 m 1274 s 1246 vw 1191 s 1074 ms	1339 m 1237 s 1180 m 1116 ms 1077 m	1340 ms 1274 ms 1235 ms 1190 s 1076 ms	1337 m 1275 ms 1275 ms 1189 ms 1117 w 1079 w	1346 w 1271 s 1237 s 1181 w 1102 m 1079 m	v(C-C) + v(C-N) CH ₂ in-plane bend
997 vw 889 s 775 ms 744 ms	1021 w 983 ms 943 w 885 ms 846 w 783 s 756 ms	1022 w 993 vw 931 vw 890 s 780 s 748 w	994 vw 939 vw 891 s 824 vw 774 s 751 vw 691 m 615 w	1025 w 997 m 939 m 894 m 818 m 781 s 757 w	δ _{rock} ; NH CH-deformation v(C-Cl); DDQ
691 w 621 ms 525 w	676 w 598 mw 564 vw 501 vw	691 mw 620 m 525 vw	579 w 502 m	667 w 608 w	skeletal vibration CH bend
430 ms	423 w	422 m	426 m	494 w 418 m	CH out of plane bend Skeletal vibration CNC def.

(a): s = strong, w = weak, m = medium, sh = shoulder, v = very, br = broad.

(b): v, stretching; δ, bending.

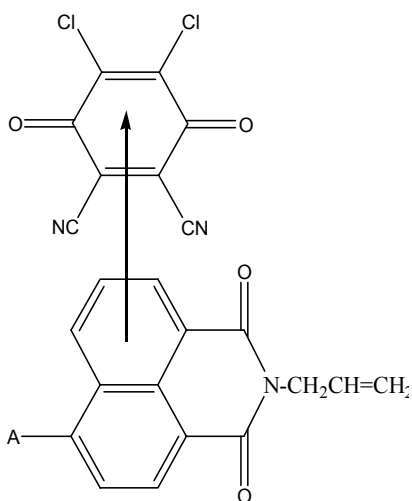
[(4PAN)(TCNQ)₂] CT complexes, the powerful electron withdrawal by CN groups in conjugation with the aromatic ring, cause a high delocalization and a great increase in the TCNQ affinity to the electron. Due to this fact, the 4MAN and 4PAN donors, which have rich donating sites (two aromatic rings, morpholine, and piperidino cyclic), are easy to be sandwiched between two TCNQ moieties to display the 1:2 stoichiometry of such CT complexes (Scheme 2). Tables 10 and 11 show the characteristic bands of CLA and

PA CT complexes. The comparison between the infrared spectral bands of the free donors and the acceptors (CLA and PA) and the corresponding bands that appear in the IR spectra of the CT complexes show the following:

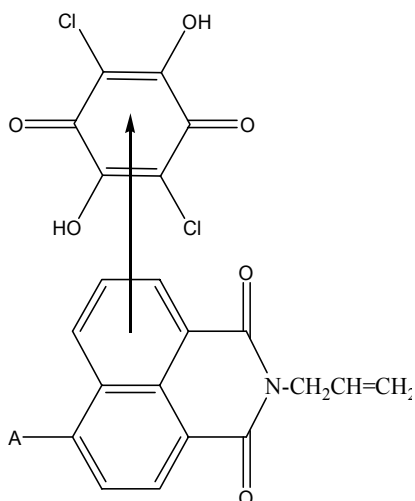
- The vibration frequency of the O-H group for the CLA and PA at 3235 cm⁻¹ and (3416 and 3103 cm⁻¹) is slightly affected in the IR spectra of the CT complexes, which means that the hydroxyl group is not involved in the CT complexation.
- The C=O group stretching vibrations, appearing at (1664 and 1630 cm⁻¹) in the case of the CLA CT complexes, are slightly shifted to

(1678 and 1637 cm^{-1}), (1632 and 1610 cm^{-1}), (1656 and 1631 cm^{-1}), (1662 and 1631 cm^{-1}) and (1630 cm^{-1}) for the 4MAN, 4PAN, 4MAAN and 4POAN, respectively. On the other hand, in the case of the picric acid, the stretching vibrations of the CT complexes of the C=O group, appearing at (1861 and 1632 cm^{-1}) are slightly shifted to (1682 and 1637 cm^{-1}), (1632 and 1610 cm^{-1}), (1699 and 1654 cm^{-1}), (1688 and 1637 cm^{-1}) and (1695, 1657 and 1632 cm^{-1}) for 4MAN, 4PAN, 4MAAN and 4POAN, respectively

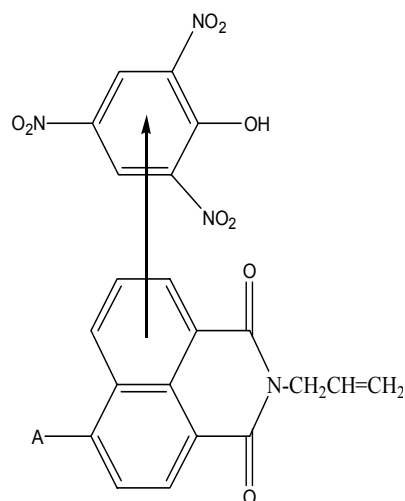
iii) The group of bands, in terms with the C-Cl vibration, which appeared at 752 and 690 cm^{-1} , exhibit a shift to a higher and a lower wavenumber in the corresponding CT complexes:



Scheme 1: The charge transfer interaction between 1,8-naphthalimide derivatives and the π -acceptor, DDQ (where A= 4-morpholino for (4MAN), 4-piperidino for (4PAN), 4-methylamino for (4MAAN), and 4-propyloxy for (4POAN)).



Scheme 2: The [(4MAN)(TCNQ)₂] and [(4PAN)(TCNQ)₂] CT complexes (where A= 4-morpholino for (4MAN) and 4-piperidino for (4PAN)).



Scheme 3: The charge transfer interaction between 1,8-naphthalimide and the π -acceptor, CLA and PA (where A= 4-morpholino for (4MAN), 4-piperidino for (4PAN), 4-methylamino for (4MAAN) and 4-propyloxy for (4POAN)).

(772 and 693 cm^{-1}), (732 and 704 cm^{-1}), (754 and 690 cm^{-1}), (755 and 688 cm^{-1}) and (756 and 695 cm^{-1}) for 4MAN, 4PAN, 4MAAN and 4POAN, respectively.

iv) The characteristic bands of the free donor, such as the stretching vibrations of the C=C, $\delta(\text{CH})$; aromatic ring, $\square(\text{C-C})$, $\square(\text{C-N})$, and the CH-deformation, are largely affected, demonstrated by their intensities. The CT complexation of N-allyl derivatives of 1,8-naphthalimide and the chloranilic acid (CLA) and picric acid (PA) occurs through π - π^* transition (from the aromatic ring of the donor to the aromatic ring of the acceptors), Scheme 3.

Mass Spectra

The mass spectrum of [(4MAAN)]₂ complex proves the complexation between 4MAAN and iodine. This becomes obvious the presence of the main fragment peaks of the donor (4MAAN), and the iodine at $m/z(\%) = 266(37\%)$ and $251(100\%)$, respectively. On the other hand, the TLC diagram, accompanying the mass spectrum, gives one sharp peak. This gives an idea about the purity of the resulted complex.

The mass spectra of the 4BAAN/TCNQ, 4MAN/TCNQ, 4PAN/TCNQ, 4MAAN/TCNQ, 4POAN/CLA, 4MAN/CLA, and 4MAAN/PA CT complexes displayed molecular ion peaks, M^+ , at

$m/z(\%)$: (308(44%) and 204(24%)) for 4BAAN and TCNQ, at (322(9%) and 204(100%)) for 4MAN and TCNQ, at (320(46%) and 204(100%)) for 4PAN and TCNQ, at (266(46%) and 204(7%)) for 4MAAN and TCNQ, at (295(37%) and 209(9%)) for 4POAN and CLA, at (322(84%) and 209(14%)) for 4MAN and CLA, and at (266(44%) and 227(2%)) for 4MAAN and PA, respectively. The intensity of these peaks gives an idea about the stability of these fragments. The presence of the molecular ion peaks of both, donor and acceptor, strongly supports the association of the charge transfer complexes of the donor and the acceptor.

Table 9. Infrared frequencies^(a) (cm⁻¹) and tentative assignments for (A): [(4BAAN)(TCNQ)]; (B): [(4MAN)(TCNQ)₂]; (C): [(4PAN)(TCNQ)₂]; (D): [(4MAAN)(TCNQ)]; and (E): [(4POAN)(TCNQ)] CT complexes.

A	B	C	D	E	Assignments ^(b)
3366 s, br 3137 w	3425 ms,br 3137 w	3425 ms, br 3136 w	3390 vs 3136 vw	3567 vw 3424 w,br 3136 vw	v(O-H); and H ₂ O of KBr v(N-H)
3050 ms	3050 ms	3050 ms	3050 ms	3050 ms	v _{as} (C-H); CH ₂ +CH ₃ v(C-H); aromatic
2957 ms 2930 ms 2866 w	2952 m 2918 vw 2847 m	2933 ms 2850 m 2810 w	2932 w 2851 vw	2964 ms 2933 w	v _s (C-H) + v _{as} (C-H)
2220 s	2221 ms	2220 s	2221 ms	2219 ms	v(C≡N); TCNQ
1683 s 1641 s	1690 s 1655 vs	1697 s 1652 vs	1680 s 1635 s	1696 s 1659 vs	v(C=O); donors
1579 vs 1542 vs	1588 s 1541 s 1512 vw	1589 ms 1541 ms 1513 vw	1576 vs 1545 vs	1589 s 1541 m 1514 mw	v(C=C); aromatic
1440 w 1421 vw 1376 s	1446 m 1379 s	1448 vw 1420 w 1381 ms	1446 m 1418 m 1380 vs	1461 ms 1380 s	δ(CH); CH _{def.} δ(CH); aromatic
1374 s 1335 s 1294 w 1246 s 1187 vw 1129 m 1100 m	1352 s 1238 s 1179 m 1152 vw 1118 s 1078 m 1021 w	1347 ms 1234 s 1177 m 1130 m 1080 m	1354 s 1298 ms 1245 ms 1154 ms 1122 vw 1089 vw 1060 vw	1328 vw 1269 s 1234 s 1183 w 1134 w 1100 ms 1077 w	v(C-C) + v(C-N) CH, in-plane bend
993 vw 934 vw 860 s 817 vw 770 ms	983 m 958 vw 917 vw 883 vw 860 s 784 ms 757 m	1020 vw 974 mw 926 vw 860 s 808 vw 780ms	1022 vw 974 vw 949 vw 861 s 814 w 771 s 655 w 652 w	1026 w 995 ms 928 ms 860 ms 833 vw 781 s 756 w	δ _{rock} ; NH CH-deformation
695 vw 662 vw	673 m 624 w 591 w 562 w	692 vw 622 mw 566 vw	581 m 521 w	668 w 625 w 551 w	skeletal vibration CH bend
474 s	498 w 474 ms	474 ms 417 m	473 ms 420 m	472 ms 410 m	CH out of plane bend Skeletal vibration CNC def.

(a): s = strong, w = weak, m = medium, sh = shoulder, v = very, br = broad.

(b): v, stretching; δ, bending.

¹HNMR Spectra

¹HNMR spectra of the 4POAN/DDQ, 4POAN/TCNQ, 4BAAN/CLA, 4PAN/CLA, 4MAAN/CLA, and 4POAN/CLA CT-complexes in DMSO were measured. It is obvious that the results from the elemental analysis, the infrared spectra, and the photometric titrations agree well with each other in the same point of ¹HNMR

spectra to interpret the mode of interaction between the donor and the acceptor. The chemical shifts (δ ppm) of the proton NMR spectra within the range of 6.5 to 8.5 peaks, assigned to the proton of the aromatic rings, were intensively affected at low intensities due to the π-π* transition.

Table 10. Infrared frequencies^(a) (cm⁻¹) and tentative assignments for (A): [(4BAAN)(CLA)]; (B): [(4MAN)(CLA)]; (C): [(4PAN)(CLA)]; (D): [(4MAAN)(CLA)]; and (E): [(4POAN)(CLA)] CT-complexes.

A	B	C	D	E	Assignments ^(b)
3508 w br 3372 s 3236 ms	3423 w br 3298 s	3510 m 3400 vw,br 3236 s	3513 ms 3390 s 3236 ms	3507 vw 3235 s	v(O-H); CLA and H ₂ O of KBr □(N-H)
--	3104 ms	3125 vw	3109 vw	3115 vw, sh	v _{as} (C-H); CH ₂ +CH ₃ v(C-H); aromatic
2957 ms 2867 w	2957 ms 2867 w	2935 m 2850 w 2815 vw	2935 vw	2966 ms 2880 w	v _s (C-H) + □ _{as} (C-H)
1678 s 1637 vs	1632 s 1610 ms	1697 m 1656 vs 1631 vs	1662 w 1631 vs	1630 vs	v(C=O); CLA donors
1580 vs 1549 s	1532 s	1592 vw 1541 w	1577 ms 1547 ms	1591 s 1543 vw 1517 m	v(C=C); aromatic
1462 w 1375 s	1430 ms	1458 w 1420 vw 1371 s	1446 w 1379 vs	1461 m 1422 vw 1380 s	δ(CH); CH _{def} δ(CH); aromatic
1338 ms 1290 w 1247 s 1186 w 1141 m 1101 m	1342 vs 1271 ms 1153 ms 1087 ms	1269 vs 1178 vw 1135 vw 1081 vw	1288 vs 1156 m 1090 vw	1272 vs 1242 vs 1170 ms 1097 ms	v(C-C) + □(C-N) CH ₂ in-plane bend
980 s 939 w 846 ms 772 ms 693 ms	919 ms 784 m 732 ms 704 ms	1019 vw 983 s 930 vw 848 s 780 ms 754 ms 690 ms	987 s 852 s 772 ms 755 m 688 ms	1027 w 978 s 927 vw 841 ms 785 s 756 ms 695 m	δ _{rock} ; NH CH-deformation v(C-Cl); CLA
572 ms 542 vw	541 w	571 s	574 ms	669 vw 569 ms	skeletal vibration CH bend
417 w	-----	420 w	422 w	462 w 410 m	CH out of plane bend Skeletal vibration CNC def.

(a): s = strong, w = weak, m = medium, sh = shoulder, v = very, br = broad.

(b): v, stretching; δ, bending.

Thermal Investigation

The thermal stability domains, the melting points, the decomposition phenomena and their assignments for the N-allyl derivatives of the 1.8-naphthalimide such as 4-Butylamino-N-allyl-1.8-naphthalimide (4BAAN), 4-Morpholino-N-allyl-1.8-naphthalimide (4MAN), 4-Piperdino-N-allyl-1.8-naphthalimide (4PAN), 4-Methylamino-N-allyl-1.8-naphthalimide (4MAAN), and 4-Propyloxy-N-allyl-1.8-naphthalimide (4POAN) CT-complexes are summarized in Table 12. The simultaneous TG/DTG curves for the 4BAAN/DDQ, 4MAN/DDQ, 4PAN/DDQ, 4MAAN/DDQ, 4POAN/TCNQ, and 4MAN/PA

(1:1) charge-transfer complexes at heating rate of 10 °C/min in static nitrogen atmosphere are given in Figure 7 (A-F).

The overall mass loss from the TG curves is 49.22% for the 4BAAN/DDQ, 63.77% for the 4MAN/DDQ, 58.08% for the 4PAN/DDQ, 41.38% for the 4MAAN/DDQ, 45.59% for the 4POAN/TCNQ, and 95.47% for the 4MAN/PA complexes, respectively. The complexes have from one to four maximal peak mass losses. The analysis of thermal curves for the CT complexes clearly indicates that the first maximum peaks are at 268, 274, 248, 150, 226, and 223°C, respectively.

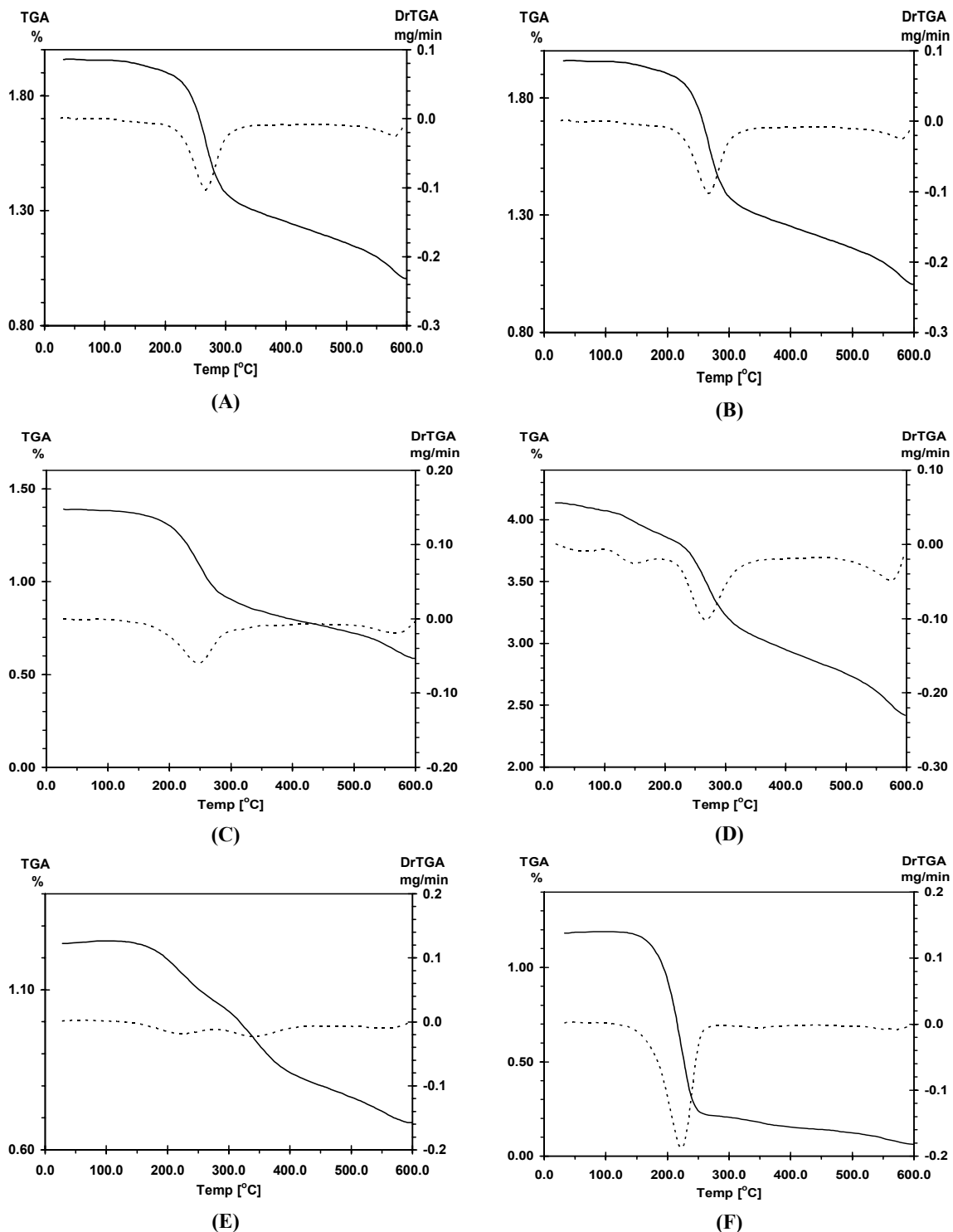


Fig. 7. TGA/DTG curves for (A): 4BAAN/DDQ; (B): 4MAN/DDQ; (C): 4PAN/DDQ; (D): 4MAAN/DDQ; (E): 4POAN/TCNQ; and (F): 4MAN/PA CT complexes.

4BAAN/DDQ CT Complex

The [(4BAAN)(DDQ)] melts at 209 °C with a simultaneous decomposition occurring. The main degradation peak is observed at 268 °C in the thermogravimetric analysis (TG) profile. Figure 7A shows the TG profile of the [(4BAAN)(DDQ)]

CT complex. It appears from the TG curve that the sample decomposes in two sharp stages in a wide temperature range of 130-600 °C. The decomposition occurs with a mass loss of 49.22%, and its calculated value is 50.65%.

Table 11. Infrared frequencies^(a) (cm⁻¹) and tentative assignments for (A): [(4BAAN)(PA)]; (B): [(4MAN)(PA)]; (C): [(4PAN)(PA)]; (D): [(4MAAN)(PA)]; and (E): [(4POAN)(PA)] CT complexes.

A	B	C	D	E	Assignments ^(b)
3365 s	3423 w,br 3297 w	3423 vw,br 3297 vw	3437 vs	3424 w,br 3299 vw	v (O-H); PA and H ₂ O of KBr v (N-H)
3102 ms	3104 ms	3102 ms	3089 ms	3102 ms	v _{as} (C-H); CH ₂ +CH ₃ v(C-H); aromatic
2956 ms 2930 m s 2868 w		2934 m 2850 vw 2813 vw	2923 vw	2967 m 2938 w 2879 w	v _s (C-H) + v _{as} (C-H)
1682 s 1637 vs	1632 s 1610 ms	1699 s 1654 s	1688 s 1637 vs	1695 s 1657 vs 1632 m	v (C=O); donors
1610 mw	1532 s	1608 ms 1541 s	1576 vs 1547 vs	1596 s 1543 s	v(C=C); aromatic v _{as} (NO ₂); PA
1580 s 1545 s 1424 ms	1430 ms	1427 ms	1423 ms 1382 s	1464 w 1425 ms 1381 w	δ(CH); CH _{def.} δ(CH); aromatic
1368 w 1340 vs 1247 s 1147 ms 1087 ms	1342 vs 1315 vw 1270 ms 1152 ms 1087 ms	1342 vs 1271 m 1235 s 1154 ms 1084 ms	1341 s 1304 ms 1242 s 1153 s 1086 ms 1060 vw	1343 s 1270 s 1237 s 1180 w 1153 m 1084 ms	v (C-C) + □(C-N) CH, in-plane bend v _s (NO ₂); PA
991 w 919 ms 821 w 771 ms 732 ms 704 ms	919 ms 784 m 732 ms 704 ms	1019 vw 975 w 918 s 851 w 781 s 731 ms	977 m 937 w 914 ms 834 w 779 ms 729 m 702 m 658 w	1025 m 994 m 919 ms 834 ms 783 s 757 w 732 m	δ _{rock} ; NH CH-deformation
580 m 522m	541 w	705 ms 541 vw	589 w 543 m	668 w 581 w 544 w	skeletal vibration CH bend
418 w	424 vw	476 vw 417 m	423 m	462 w 410m	CH out of plane bend Skeletal vibration CNC def. δ(ONO); PA

(a): s = strong, w = weak, m = medium, sh = shoulder, v = very, br = broad.

(b): v, stretching; δ, bending.

4MAN/DDQ CT Complex

The thermal analysis curves for the 4MAN/DDQ CT complex show that decomposition takes place in a single stage in a temperature range between 150 and 600 °C at maximum differential thermogravimetric analysis (DTG_{max}) of 274 °C (Figure 7 B). The single endothermic decomposition stage corresponds to the decomposition of both, the donor and the acceptor (DDQ). The TG curve of the [(4MAN)(DDQ)] complex shows a weight loss

(Found 63.77, Calcd. 65.03%) corresponding to the loss of organic moiety, C₁₁H₁₈N₄O₅Cl₂. The final product, formed at 600 °C, consists of limited 16C with insufficient oxygen atoms.

4PAN/DDQ CT Complex

The thermal degradation of the [(4PAN)(DDQ)] CT-complex proceeds in two main stages (Figure 7C). These two stages relate to the decomposition of the 4-Piperdino-N-allyl-1.8naphthalimide (4PAN) and the DDQ as an acceptor; (Found 58.08%; Calcd. 58.32%), in

Table 12: Thermal data of: (A): 4BAAN/DDQ; (B): 4MAN/DDQ; (C): 4PAN/DDQ; (D): 4MAAN/DDQ; (E): 4POAN/TCNQ; and (F): 4MAN/PA CT complexes.

Complexes	Steps	Temp/range (°C)	DTG _{max}	TG		Assignments
				Total weight loss (%)		
				Found	Calc.	
A	1 st	130-475	268	49.22	50.65	C ₅ H ₂₀ N ₄ O ₄ Cl ₂ 22C Residue
	2 nd	475-600	581			
B	1 st	150-600	274	63.77	65.03	C ₁₁ H ₁₈ N ₄ O ₅ Cl ₂ 16C Residue
C	1 st	70-325	248	58.08	58.32	C ₉ H ₂₀ N ₄ O ₄ Cl ₂ 19C Residue
	2 nd	325-600	570			
D	1 st	25-80	61	41.38	41.58	H ₁₄ N ₄ O ₄ Cl ₂ 24C Residue
	2 nd	80-200	150			
	3 rd	200-350	269			
	4 th	350-600	576			
E	1 st	150-250	226	45.59	47.09	C ₈ H ₂₁ N ₅ O ₃ 22C Residue
	2 nd	250-400	343			
	3 rd	400-600	560			
F	1 st	130-280	223	95.47	95.64	C ₂₃ H ₂₁ N ₅ O ₁₃ 2C Residue
	2 nd	280-400	352			
	3 rd	400-600	561			

temperature ranges of 70-600 °C by giving an endothermic effect (DTG_{max}: 248 and 570 °C).

4MAAN/DDQ CT Complex

The TG diagrams of the [(4MAAN)(DDQ)] CT complex reveal mass loss in the temperature range of 25-600°C, corresponding to the formation of residual carbon atoms due to a limited supply of oxygen. The four endothermic peaks are observed in the DTG analysis (Figure 7D). The maxima of these peaks are found to be (DTG_{max}: 61, 150, 269, and 576°C). The first peak is referring to the melting point of the CT complex. This step occurred without mass loss and it can be assigned any organic moiety. The mass losses at 150, 269, and 579°C DTG_{max}, respectively, are endothermic decompositions and correspond to the loss of the H₁₄N₄O₄Cl₂ organic rest. The overall weight loss (Found 41.38%, calcd. 41.58%) agrees well with the proposed structure.

4POAN/TCNQ CT Complex

The TG of the [(4POAN)(TCNQ)] CT complex: three steps are shown in the pyrolysis curve at 226, 343 and 560 °C. The first step corresponds to the eliminated C₃H₆O molecule (Calcd.: 11.62%, Found: 12.26%). The remaining two, the TCNQ and the 1.8naphthalimide molecules, decompose in the second and the third steps with the formation of 22C as the final residue.

4MAN/PA CT Complexes

The 4MAN/PA CT complex consists of three decomposition steps at 223, 352, and 561 °C. The

first step, which is in the 130-280°C temperature range, corresponds to the decomposition of both, the donor (4MAN) and the acceptor (PA) (C₂₃H₂₁N₅O₁₃, organic moiety), in the presence of oxygen atoms, gave 83.16% weight loss. The second and the third steps (DTG_{max}; 352 and 561°C) seems to be consistent with the evolution of the CO (Calcd.: 5.08%, Found: 4.61%), and the CO₂ (Calcd.: 7.98%, Found: 7.70%) molecules, respectively.

Kinetic Studies

The kinetic data of the first and the second decomposition steps of the 4BAAN/DDQ, 4MAN/DDQ, 4PAN/DDQ, 4MAAN/DDQ, 4POAN/TCNQ, and 4MAN/PA CT complexes was presented using the Coats-Readfern and Horowitz-Metzger methods [31,32]. The kinetic parameters, E, A, ΔS, ΔH, ΔG, and r, is calculated and the data are listed in Table 13.

The activation energies of the formation of 1.8-naphthalimide derivatives with DDQ in the case of the first degradation step are in the following order:



The comparison between 4POAN/TCNQ and 4MAN/PA found that the activation energy in the TCNQ complex is higher five times than in the PA charge-transfer complex due to the strong powerful TCNQ acceptor, which contains four cyano groups.



Table 13: Kinetic parameters, obtained through the Coats–Redfern (CR) and Horowitz–Metzger (HM) methods for (A): 4BAAN/DDQ; (B): 4MAN/DDQ; (C): 4PAN/DDQ; (D): 4MAAN/DDQ; (E): 4POAN/TCNQ; and (F): 4MAN/PA CT complexes.

complex	stage	method	parameter					r
			E (Jol ⁻¹)	A (s ⁻¹)	ΔS (J mol ⁻¹ K ⁻¹)	ΔH (J mol ⁻¹)	ΔG (J mol ⁻¹)	
A	1 st	CR	1.11×10 ⁵	4.06×10 ⁸	-8.49×10 ¹	1.06×10 ⁵	1.52×10 ⁵	0.9989
		HM	1.19×10 ⁵	5.57×10 ⁹	-6.32×10 ¹	1.14×10 ⁵	1.48×10 ⁵	0.9978
		average	1.15×10 ⁵	2.31×10 ⁸	-7.41×10 ¹	1.10×10 ⁵	1.5×10 ⁵	
	2 nd	CR	3.49×10 ⁵	3.91×10 ¹⁹	1.21×10 ²	3.42×10 ⁵	2.38×10 ⁵	0.9961
		HM	3.69×10 ⁵	5.54×10 ²⁰	1.43×10 ²	3.61×10 ⁵	2.39×10 ⁵	0.9988
		average	3.59×10 ⁵	2.232×10 ¹⁹	1.32×10 ²	3.51×10 ⁵	2.39×10 ⁵	
B	1 st	CR	7.7×10 ⁴	1.49×10 ⁵	-1.51×10 ²	7.24×10 ⁴	1.55×10 ⁵	0.9977
		HM	8.59×10 ⁴	1.32×10 ⁵	-1.33×10 ²	8.13×10 ⁴	1.54×10 ⁵	0.9984
		average	8.15×10 ⁴	1.41×10 ⁵	-1.42×10 ²	7.68×10 ⁴	1.55×10 ⁵	
C	1 st	CR	6.4×10 ⁴	1.30×10 ⁴	-1.71×10 ²	5.97×10 ⁴	1.49×10 ⁵	0.9996
		HM	7.18×10 ⁴	1.16×10 ⁴	-1.53×10 ²	6.74×10 ⁴	1.47×10 ⁵	0.9981
		average	6.79×10 ⁴	1.23×10 ⁴	-1.62×10 ²	6.36×10 ⁴	1.48×10 ⁵	
	2 nd	CR	2.33×10 ⁵	3.21×10 ¹²	-1.41×10 ¹	2.26×10 ⁵	2.38×10 ⁵	0.9999
		HM	2.31×10 ⁵	2.12×10 ¹²	-1.76×10 ¹	2.24×10 ⁵	2.39×10 ⁵	0.9996
		average	2.32×10 ⁵	2.67×10 ¹²	-1.58×10 ¹	2.25×10 ⁵	2.39×10 ⁵	
D	1 st	CR	4.73×10 ⁴	1.4×10 ⁵	-1.47×10 ²	4.46×10 ⁴	9.36×10 ⁴	0.9936
		HM	5.17×10 ⁴	1.82×10 ⁶	-1.26×10 ²	4.9×10 ⁴	9.1×10 ⁴	0.9973
		average	4.95×10 ⁴	0.791×10 ⁵	-1.37×10 ²	4.68×10 ⁴	9.23×10 ⁴	
	2 nd	CR	5.04×10 ⁴	4.98×10 ³	-1.77×10 ²	4.68×10 ⁴	1.22×10 ⁵	0.9998
		HM	5.84×10 ⁴	1.56×10 ⁵	-1.48×10 ²	5.48×10 ⁴	1.18×10 ⁵	0.9981
		average	5.44×10 ⁴	2.49×10 ³	-1.63×10 ²	5.08×10 ⁴	1.2×10 ⁵	
E	1 st	CR	5.71×10 ⁴	5.01×10 ³	-1.78×10 ²	5.3×10 ⁴	1.42×10 ⁵	0.9893
		HM	6.23×10 ⁴	2.6×10 ⁴	-1.65×10 ²	5.82×10 ⁴	1.4×10 ⁵	0.9997
		average	5.97×10 ⁴	2.64×10 ³	-1.72×10 ²	5.56×10 ⁴	1.41×10 ⁵	
	2 nd	CR	7.9×10 ⁴	2.16×10 ⁴	-1.68×10 ²	7.4×10 ⁴	1.77×10 ⁵	0.9854
		HM	8.75×10 ⁴	1.98×10 ⁵	-1.5×10 ²	8.24×10 ⁴	1.74×10 ⁵	0.9992
		average	8.33×10 ⁴	2.07×10 ⁴	-1.59×10 ²	4.82×10 ⁴	1.76×10 ⁵	
F	1 st	CR	1.01×10 ⁵	6.18×10 ⁸	-8.09×10 ¹	9.74×10 ⁴	1.38×10 ⁵	0.9988
		HM	1.11×10 ⁵	5.45×10 ⁹	-6.28×10 ¹	1.07×10 ⁵	1.38×10 ⁵	0.9999
		average	1.06×10 ⁵	30.3×10 ⁸	7.19×10 ¹	10.2×10 ⁴	1.38×10 ⁵	
	2 nd	CR	1.16×10 ⁵	3.64×10 ⁷	-1.06×10 ²	1.11×10 ⁵	1.77×10 ⁵	0.9985
		HM	1.29×10 ⁵	6.60×10 ⁸	-8.22×10 ¹	1.24×10 ⁵	1.75×10 ⁵	0.9983
		average	1.23×10 ⁵	34.8×10 ⁷	-9.41×10 ¹	1.18×10 ⁵	1.76×10 ⁵	

REFERENCES

1. E. Martin, R. Weigand, A.Pardo, *J. Lumines.*, **68**, 157 (1996).
2. V. Gruzinskii, A. Kukhta, G. Shakkah, *J. Appl. Spectr.*, **65**, 444 (1998).
3. Z-F. Tao, X. Qian, *Dyes and Pigments*, **43**, 139 (1999).
4. K. Dubey, R. Singh, K. Mizra, *Indian J. Chem.*, **34B**, 876 (1995).
5. M. M. de Souza, R. Correa, V. Cechinel Filho, I. Grabchev, V. Bojinov, *Pharmazie*, **56**, 75 (2002).
6. A. D. Andricopulo, R.A. Yunes, V. Cechinel Filho, R. Correa, A.W. Filho, A.R. Santos, R.J. Nunes, *Acta Farm. Bonaerenses*, **17**, 219 (1998).
7. X. Qian, K. Zhu, K. Chen, *Dyes and Pigments*, **11**, 13 (1989).
8. E. Wolarz, H. Moryson, D. Bauman, *Displays*, **13**, 171 (1992).
9. E. Mykowska, K. Jazwanska, W. Grupa, D. Bauman, *Proc SPIE* **3318**, 378 (1998).
10. I. Grabchev, I. Moneva, E. Wolarz, D. Bauman, *Z Naturforsch.*, **51a**, 1185 (1996).
11. S. K. Das, G. Krishnamoorthy and S. K. Dofra, *Can. J. Chem.*, **78**, 191 (2000).
12. G. Jones, J. A. C. Jimenez, *Tetrahedron Lett.*, **40**, 8551(1999).
13. G. Smith, R. C. Bott, A. D. Rae, A. C. Willis, *Aust. J. Chem.*, **53**, 531 (2000).
14. G. Smith, D. E. Lynch, R. C. Bott, *Aust. J. Chem.*, **51**, 159 (1998).
15. G. Smith, D. E. Lynch, K. A. Byriel, C. H. L. Kennard, *J. Chem. Crystallogr.*, **27**, 307 (1997).
16. M.S. Refat, S. A. Sadeek, H.M. Khater, *Spectrochim. Acta Part A*, **64(3)**, 778 (2006).
17. M.S. Refat, A.M. El-Didamony, *Spectrochim. Acta Part A*, **65(3-4)**, 732 (2006).

18. M.S. Refat, I. Grabchev, J.-M. Chovelon, G. Ivanova, *Spectrochim. Acta Part A*, **64(2)**, 435 (2006).
19. M.S. Refat, H. Al-Didamony Ahmed, L.A. El-Zayat, *Can. J. Anal. Sci. Spec.*, **51(3)**, 147 (2006).
20. M.S. Refat, H.M.A. Killa, I. Grabchev, M.Y. El-Sayed, *Spectrochim. Acta Part A*, **68(1)**, 123 (2007).
21. M.S. Refat, L.A. El-Zayat, Okan Zafer Yeşilel, *Polyhedron*, **27(2)**, 475 (2008).
22. M.S. Refat, H.A. Ahmed, I. Grabchev, L.A. El-Zayat, *Spectrochim. Acta*, **70(4)**, 907 (2008).
23. M.S. Refat, L.A. El-Zayat, Okan Zafer Yeşilel, *Spectrochimica Acta Part A*, **75**, 745 (2010).
24. M.S. Refat, Hamdy Al. Didamony, Khlood M. Abou El-Nour, I. Grabchev, Lamia El-Zayat, *Arab. J. Chem.*, in press.
25. 25 (a) I. Grabchev, Ch. Petkov, and V. Bojinov, *Dyes and Pigments*, **48**, 239 (2001); (b) T Konstantinova, P. Meallier, I. Grabchev, *Dyes and Pigments*, **22**, 191 (1993); (c) I. Grabchev, T Konstantinova, P. Meallier, M. Popova, *Dyes and Pigments*, **28**, 41 (1995).
26. F. M. Abou Attia, *Farmaco*, **55**, 659 (2000).
27. D. A. Skoog, *Principle of Instrumental Analysis*, 3rd edn., Saunders College Publishing, New York, USA, 1985, Ch. 7.
28. R. Abu-Eittah, F. Al-Sugeir, *Can. J. Chem.*, **54**, 3705 (1976).
29. G. G. Aloisi, S. Pignataro, *J. Chem. Soc., Faraday Trans.*, **69**, 534 (1973).
30. A. El-Kourashy, *Spectrochim. Acta.*, **37A**, 399 (1981).
31. A.W. Coats, J.P. Redfern, *Nature*, **201**, 68 (1964).
32. H.W. Horowitz, G. Metzger, *Anal. Chem.*, **35**, 1464 (1963).

СИНТЕЗИ И ХАРАКТЕРИЗИРАНЕ НА КОМПЛЕКСИ С ПРЕНОС НА ЗАРЯДА НА 1,8-НАФТАЛИМИДИ С РАЗЛИЧНИ АКЦЕПТОРИ

М.С. Рефат^{a,b}, Х.А. Дидамони^c, Х.М. Абу Ел-Нур^d,
И. Грабчев^e, Л. Ел-Заят^a

^aДепартамент по химия, Факултет за наука, Университет в Порт Сауд, Порт Сауд 42111, Египет

^bДепартамент по химия Факултет за наука, Университет в Тауиф, 888 Тауиф, Кралство Саудитска Арабия

^cДепартамент по химия Факултет за наука, Университет в Загазиг, Загазиг, Египет

^dДепартамент по химия Факултет за наука, Университет "Суецки канал", Исмаилия, Египет

^eФакултет по медицина, Софийски университет "Св. Климент Охридски" ул. Козяк 1, 1407 София, България

Постъпила на 24 април, 2010 г.; преработена на 7 юли, 2010 г.

(Резюме)

При взаимодействието на донори (4-заместени-N-алил-1,8-нафталиמידни производни), и σ -акцептори (йод или π -акцептори) са получени пет нови комплекса с пренос на заряда (КПЗ) и детайлно са изследвани функционалните им характеристиките. Показано е, че се образуват комплекси с пренос на заряда с общи формули: [(донор)(акцептор)_n], при n= 1 в случая на комплексите [(донори)I₂], [(донори)(DDQ)], [(донори)(CLA)], [(донори)(PA)] и [(донори)(TCNQ)] докато при n = 2 комплексите са [(4MAN)(TCNQ)₂], и [(4PAN)(TCNQ)₂].